doi:10.3772/j.issn.1006-6748.2024.02.008

Heat dissipation enhancement method for finned heat sink for AGV motor driver's IGBT module[①]

LIU Xuan(刘 璇)[②], ZHANG Mingchao, LIU Chengwen, ZHOU Chuanan, LV Xiaoling
(School of Mechanical Engineering, Hebei University of Technology, Tianjin 300401, P. R. China)

Abstract

With the widespread use of high-power and highly integrated insulated gate bipolar transistor (IGBT), their cooling methods have become challenging. This paper proposes a liquid cooling scheme for heavy-duty automated guided vehicle (AGV) motor driver in port environment, and improves heat dissipation by analyzing and optimizing the core component of finned heat sink. Firstly, the temperature distribution of the initial scheme is studied by using Fluent software, and the heat transfer characteristics of the finned heat sink are obtained through numerical analysis. Secondly, an orthogonal test is designed and combined with the response surface methodology to optimize the structural parameters of the finned heat sink, resulting in a 14.57% increase in the heat dissipation effect. Finally, the effectiveness of heat dissipation enhancement is verified. This work provides valuable insights into improving the heat dissipation of IGBT modules and heat sinks, and provides guidance for their future applications.

Key words: finned heat sink, insulated gate bipolar transistor (IGBT) module, heat dissipation, orthogonal test, response surface methodology

0 Introduction

Automated guided vehicle (AGV) is critical components of modern logistics transportation systems and represents an important research direction for future automated ports[1-2]. The design, operation, and maintenance of AGV systems have attracted considerable attention from academic and industrial communities[3]. The motor driver is a crucial control component of AGV, with the insulated gate bipolar transistor (IGBT) module inside generating significant heat due to constraints in heat dissipation space and packaging structure. This phenomenon is particularly severe in heavy-duty AGV operating in port environments[4]. Therefore, studying methods to avoid IGBT module overheating and failure is crucial.

Extensive research has been conducted on the design of IGBT module packaging, heat dissipation structures, and heat dissipation enhancement[5-10]. Huo et al.[11] designed a battery thermal management system based on microchannels and studied the influence of factors such as channel quantity, flow direction, inlet mass flow rate, and environmental temperature on temperature rise and distribution during battery discharge. Xu et al.[12] studied the pressure distribution of cooling medium and the temperature distribution of chip and heat sink under different conditions based on the double-sided forced liquid-cooled packaging structure of high-power IGBT module. Xiahou et al.[13] optimized the structure of traditional gravity heat pipes and designed a new array cold-end flat plate heat pipe. Based on the correlation analysis and Kriging method, Song et al.[14] constructed the response surface model. And based on the archive based micro genetic algorithm (AMGA), the multi-objective optimization of the internal channel structure of the water-cooled heat sink was cared out. Lampio and Karvinen[15] introduced a method for calculating the temperature field and heat transfer of forced or natural convection-cooled heat sinks, which was suitable for multi-objective optimization.

Despite the extensive research that has been conducted, there is still a lack of study on liquid cooling of high-power IGBT modules. In addition, the structur-

① Supported by the National Key Research and Development Plan Program (No. 2022YFB4701101), National Natural Science Foundation of China (No. U1913211) and Natural Science Foundation of Hebei Province of China (No. F2021202062).
② To whom correspondence should be addressed. E-mail: xuaner1007@163.com.
Received on May 22, 2023

al parameter optimization research based on heat transfer characteristics is insufficient, and there is a lack of research on multi-parameter combination optimization of interactive variables. Therefore, this paper focuses on the heavy-duty AGV motor driver in port environments, and proposes a liquid cooling scheme, analyzes and optimizes the heat dissipation core component—finned heat sink—based on heat transfer characteristics. By doing so, the heat dissipation effect has increased by 14.57%, meeting the requirement for maximum junction temperature.

1 Design and simulation analysis of liquid cooling scheme

1.1 Design of the liquid cooling scheme

The AGV motor driver studied in this paper has the following operating conditions: (1) workspace dimensions are 760 mm × 420 mm × 300 mm; (2) IGBT module's working power: 1.2 kW; (3) maximum allowable temperature is 80 ℃; (4) working environment temperature range is −30 – 50 ℃; (5) the equipment requires a sealed design.

The prevailing cooling methods for IGBTs in the market are air cooling, liquid cooling, and phase-change material cooling. Air cooling utilizes convection heat transfer between the heat sink and the surrounding air, offering ease of implementation but limited heat dissipation efficiency. Liquid cooling employs a specific coolant as the heat transfer medium, providing notable advantages in heat dissipation effectiveness and temperature uniformity. Phase-change material cooling utilizes the heat absorption during phase transition to lower the temperature. However, phase-change materials lack inherent heat dissipation capacity and rely solely on their ability to absorb and store heat during phase transition for heat dissipation. In practical engineering applications, air cooling and liquid cooling are the most common methods. Considering the motor driver's operation in a high-temperature and humid port environment, and the need for sealed electronic devices, liquid cooling is better suited for efficient heat dissipation.

The ambient temperature is set to 45 ℃ to ensure the reliability of the scheme, and is the maximum junction temperature calculated by derating at $0.85\,T_{\max}$. Therefore, the maximum allowable junction temperature for the IGBT module is 68 ℃. The liquid cooling scheme for the motor driver is designed, and the overall layout structure is shown in Fig. 1. Throughout the cooling process, the finned heat sink is the core component.

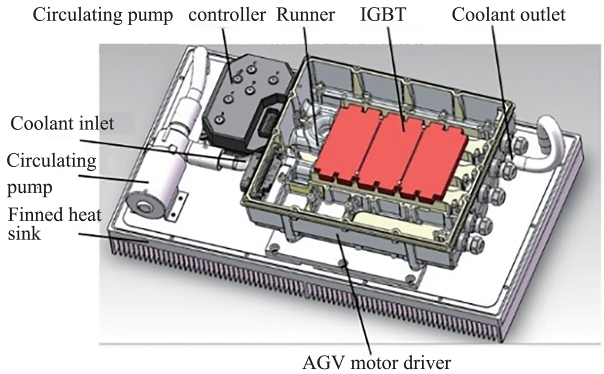

Fig. 1 Schematic diagram of the liquid cooling scheme of the motor driver

The finned heat sink consists of a substrate and fins. This paper uses rectangular fins and series flow channel structure of the substrate, which balances maintenance convenience, processing costs, and heat dissipation characteristics. The structure of the finned heat sink is shown in Fig. 2, and the initial model parameters are listed in Table 1.

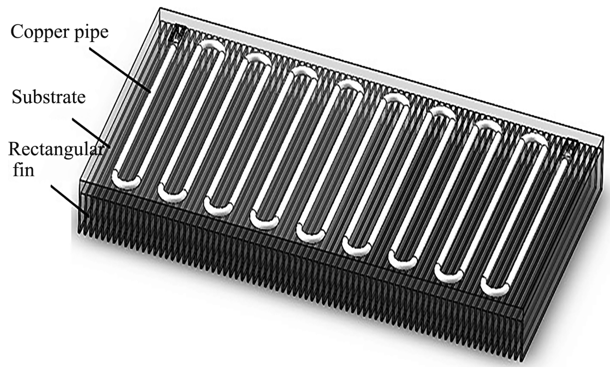

Fig. 2 Finned heat sink structure

Table 1 Finned heat sink model parameters

Structural parameters	Size
Fin height/mm	45
Fin thickness/mm	2
Substrate thickness/mm	15
Number of fins/mm	80
Finned heat sink length/mm	740
Finned heat sink width/mm	350

1.2 Simulation analysis of the liquid cooling scheme

The simulation analysis is shown in Fig. 3, the current cooling system design fails to meet the IGBT module's cooling requirements as it exceeds the maximum temperature limit of 68 ℃ in steady-state. Therefore, optimization is necessary to improve the cooling system's effectiveness. From the direction of structure optimization, the heat dissipation effect of the finned heat sink can be enhanced.

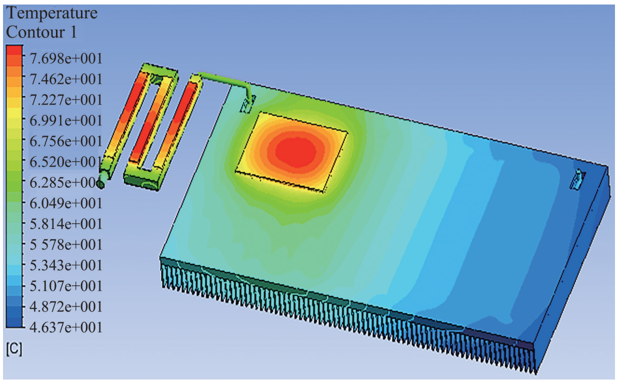

(a) Temperature field distribution of liquid cooling scheme

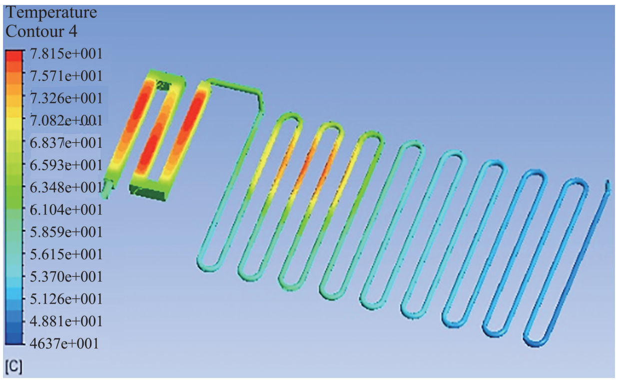

(b) Temperature field distribution of coolant

Fig. 3 Temperature field distribution

1.3 Influence of structural parameters of the finned heat sink on the junction temperature of the IGBT module

To optimize the structure of the finned heat sink, it is necessary to investigate the impact of structural parameters on its thermal performance. Therefore, a parametric model is established in Fluent by using the control variable method, with structural parameters as variables. Simulation results from each parameter model are used to establish the relationship between the maximum temperature of the IGBT module and the various parameters, as shown in Fig. 4.

To balance the heat dissipation effect and material cost of the fin, this paper sets the range of the number of fins (N) as $77 \leqslant N \leqslant 81$, the range of the fin thickness (δ) as $2.5 \leqslant \delta \leqslant 4.0$, and the range of the fin height (h) as $40 \leqslant h \leqslant 55$. For the sake of convenience, the thickness of the substrate is selected as 24 mm, which lays the foundation for subsequent structural optimization.

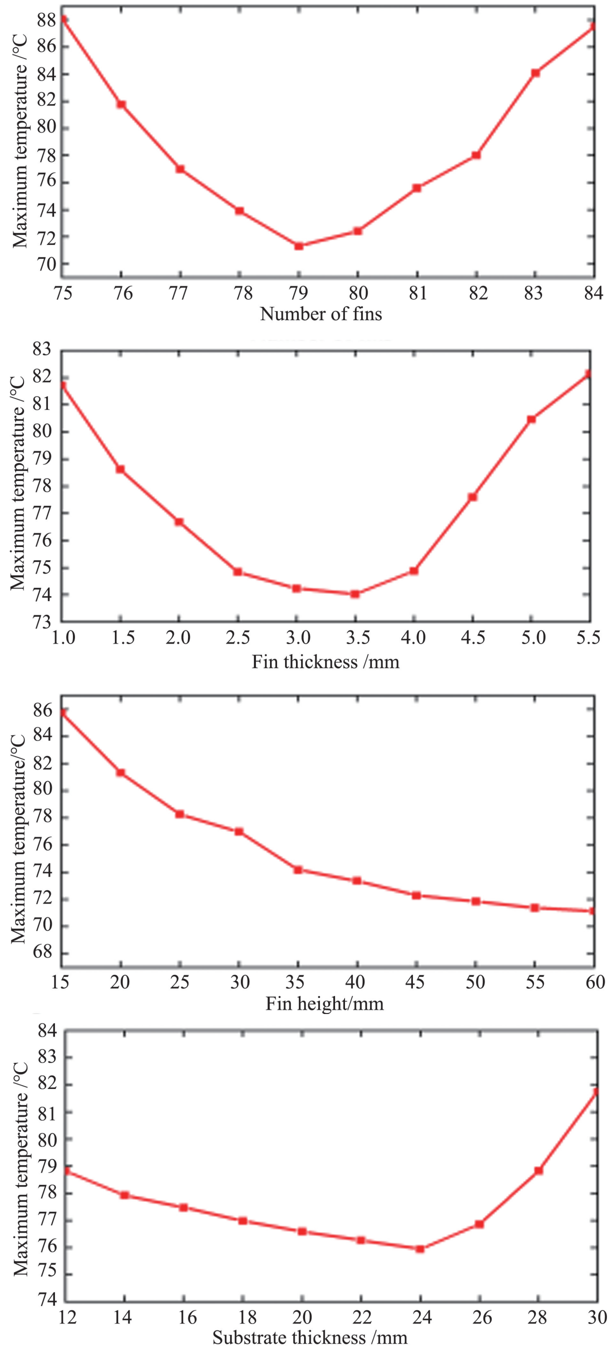

Fig. 4 Relationship between the structural parameters and maximum temperature of the IGBT module

2 Numerical analysis of the finned heat sinks

2.1 Analysis of heat transfer model for rectangular fins

Analyzing the heat transfer model of finned heat sinks from the perspective of heat transfer theory can establish a foundation for subsequent optimization work. It is assumed that L, W, and H are the length, width, and height of the finned heat sink, respectively; and N, p, δ, h, and b are the number of fins and the spacing between fins, fin thickness, fin height, substrate thickness, respectively. Taking a single fin as the analysis object, its structural parameters on the heat transfer wall are shown in Fig. 5 (a). Suppose the heat transfer of the fin is steady-state heat transfer; the temperature of the fin root is t_0, the temperature of the surrounding fluid is t_1, and the cross-sectional area of the fin is A_c. Fig. 5(b) is a cross-sectional view of the single-fin heat transfer model, taking a micro-element segment dx as the research object and treating it as a steady-state heat transfer system, and setting the heat energy transferred into and out of the micro-element segment per unit time as Φ_x, Φ_{x+dx}, the heat energy of the convective heat exchange between the outer surface of the micro-element section and the air is Φ_c, and the volume of the micro-element section is $A_c dx$.

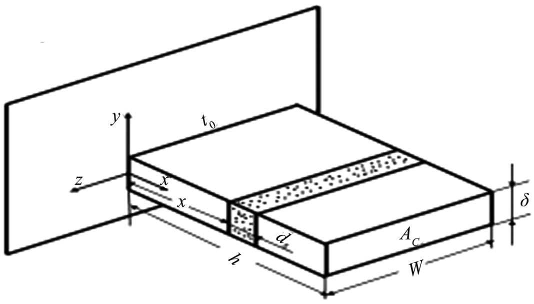

(a) Schematic diagram of structure

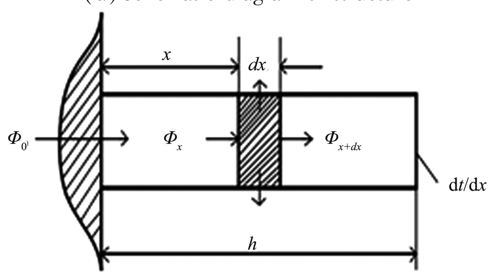

(b) Sectional view of heat transfer model

Fig. 5 Schematic diagram of the single fin

According to the law of conservation of energy:

$$\Phi_x = \Phi_{x+dx} + \Phi_c \tag{1}$$

According to the heat conduction equation, it can be known:

$$\Phi_x = -k_{Al}A_c\frac{\mathrm{d}t}{\mathrm{d}x} \tag{2}$$

$$\Phi_{x+dx} = \Phi_x + \frac{\mathrm{d}\Phi_x}{\mathrm{d}x} = \Phi_x - k_{Al}A_c\frac{\mathrm{d}^2t}{\mathrm{d}x^2}\mathrm{d}x \tag{3}$$

where k_{Al} is the ther malconductivity of the fin.

From the convection heat transfer formula, it can be known that:

$$\Phi_c = k_f U dx(t - t_1) \tag{4}$$

where k_f is the convective heat trassfer coefficciest of the fin surface, U is the perimmeter of the fin.

Substituting Eqs (3) and (4) into Eq. (1), the differential equation for heat transfer with fins can be derived:

$$\frac{\mathrm{d}^2t}{\mathrm{d}x^2} - \frac{k_fU}{k_{Al}A_c}(t - t_1) = 0 \tag{5}$$

The temperature distribution function of the rectangular fin along the height direction is obtained by

$$t = t_0 + \frac{\cosh[m(h - x)]}{\cosh(mh)} \tag{6}$$

where, $m = \sqrt{\frac{k_f u}{k_f A_c}}\cosh(x) = \frac{e^x + e^{-x}}{2}$. Substituting Eq. (6) into Fourier's law can deduce the heat transfer of rectangular fins:

$$\Phi = \frac{k_fU}{m}\cdot\theta_0\cdot\tanh(mh) \tag{7}$$

where $\theta_0 = t_0 - t_1$.

In actual engineering, the heat taken away by the factor of fin thickness is negligible. If thicker fins are used, $h_c = h + \delta/2$ can be used to approximate the fin height. The fin efficiency for rectangular fins can be written as

$$\eta_f = \frac{\frac{k_fU}{m}\cdot\theta_0\cdot\tanh(mh)}{k_fUh\theta_0} = \frac{\tanh(mh)}{mh} \tag{8}$$

From Eq. (8), the efficiency of rectangular fins is a function of (mh). Assuming that the fin thickness δ is much smaller than the fin length W, taking the fin of unit length, the perimeter U of the cross-section of the fin is 2, mh can be simplified as

$$mh = \sqrt{\frac{k_fU}{k_{Al}A_c}}\cdot h = \sqrt{\frac{2k_f}{k_{Al}\delta}}\cdot h = \sqrt{\frac{2k_f}{k_{Al}A_L}}\cdot h^{\frac{3}{2}} \tag{9}$$

where, $A_L = \delta h$, which represents the cross-sectional area of the rectangular fin.

The thermal analysis presented above focuses on individual fins and only considers the heat transfer between the outer surface of a single fin and the surrounding air. However, in reality, fins of the finned heat sink are used in groups. Therefore, convective heat transfer consists of two main parts: one is the heat transfer between the outer surface of each fin and the surrounding air, and the other is the heat transfer between the outer surface of the substrate not blocked by the fin root and the air. The temperature of the outside air is t_1, the convective heat transfer coefficient between the air and the entire outer surface is k_f, the surface area of the fins is A_{fin}, and the outer surface area of the substrate between the roots of adjacent fins is A_{base}, so the total heat transfer area of the finned heat sink is $A_0 = A_{fin} + A_{base}$. The outer surface temperature of the root of the fin and the substrate are both t_0. The total heat transfer from convection between air and fins can be calculated using the fin thermal conductivity formula and fin efficiency formula.

$$\begin{aligned}\Phi &= A_{base} k_f (t_0 - t_1) + A_{fin} \eta_f k_f (t_0 - t_1) \\ &= A_0 \eta_0 k_f (t_0 - t_1)\end{aligned} \tag{10}$$

where, $\eta_0 = \dfrac{A_{base} + A_{fin}\ \eta_f}{A_{base} + A_{fin}}$.

Based on the analysis above, it can be concluded that the heat dissipation efficiency of fins is a function of mh and depends on the material's thermal conductivity, convective heat transfer coefficient between the fin and the surrounding air, and the fin's geometry. To enhance the heat dissipation effect, one can employ methods such as selecting materials with high thermal conductivity, installing forced air-cooling devices, or choosing an appropriate fin structure. Moreover, from the multi-finned surface heat transfer model analysis, researchers found that the influence of the number of fins on the total heat transfer mainly depended on two factors: the contact area between all fins and the base, and the spacing between fins. Adjusting the number of fins can enhance heat dissipation, but there is an inevitable constraint between the number of fins and their spacing. Therefore, how to balance the optimal data to ensure the best heat dissipation effect is a problem that needs to be addressed.

2.2 Heat transfer characteristics of the fin

By using Matlab to solve the heat transfer differential equations of fins the heat transfer process of fins can be simulated and analyzed, and then the heat transfer characteristics of fins can be obtained. Assume that the thickness δ of the rectangular fin is much smaller than the length W, the fin of unit length is taken along the height direction, the perimeter U of the cross-section of fin is 2, and the cross-sectional area A_c is δ. According to the heat transfer differential equation (Eq. (5)), it can be got:

$$\frac{d^2 t}{dx^2} \cdot \delta = \frac{2k_f}{k_{Al}} \cdot (t - t_1) \tag{11}$$

According to the boundary conditions, Eq. (11) can be transformed into a first-order ordinary differential equation:

$$\begin{cases} y'_1 = y_2 \\ y'_2 = \dfrac{2k_f(y_1 - t_1)}{k_{Al}\delta} - \dfrac{y_2}{x} \\ y_1(x_1) = t_0, y_2(x_2) = 0, x_1 < x < x_2 \end{cases} \tag{12}$$

Based on the simulation results presented earlier, the Runge-Kutta method in the Matlab solver can solve Eq. (12)[16]. The relationship curve between heat dissipation $\Phi(W)$, fin thickness δ, and fin height h is shown in Fig. 6.

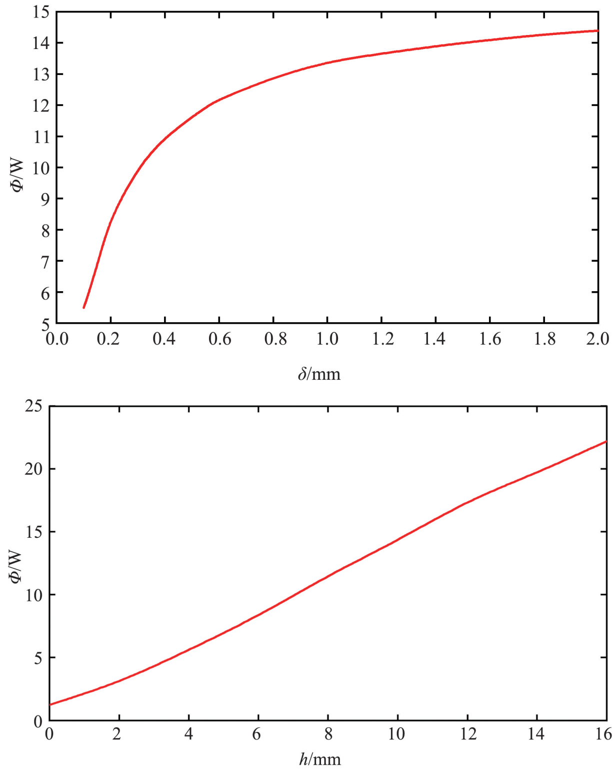

Fig. 6 Relationship between heat dissipation and thickness of fins and fin height

From Fig. 6, it can be seen that the height of the fin has a more significant impact on heat dissipation. The mathematical heat transfer model of the fin indicates that several factors, such as surface heat transfer coefficient, fin height, and fin thickness, affect its heat dissipation performance. Additionally, Section 1 reveals the significance of factors such as the number of fins and substrate thickness in optimizing the design. However, there may exist nonlinear constraints between these factors. Therefore, orthogonal experimental design can be used to analyze and screen out important factors, and response surface methodology can be used for optimization[17-23].

3 Structural parameter optimization of the finned heat sink

3.1 Orthogonal test design

An orthogonal test design with seven factors and two levels is conducted to compare the influence of different factors on heat dissipation performance, as shown in Table 2. Based on the eight parameter combinations designed according to the orthogonal test principle, the maximum temperature of the IGBT module is calculated using Fluent, and the specific results are shown in Table 3 and Fig. 7.

Table 2 Orthogonal test factor level table

Factor	Level 1	Level 2
A: Cooling medium flow rate/m · s^{-1}	1.2	1.8
B: Fin height/mm	42	50
C: Number of fins	76	82
D: Fin thickness/mm	2.6	3.8
E: Substrate thickness/mm	18	24
F: Heat sink material/(W · m^{-1} · K^{-1})	218	385
G: Ambient temperature/℃	30	40

Table 3 Seven-factor two-level orthogonal test scheme

	A	B	C	D	E	F	G	T_{max}/℃
1	2	2	2	2	2	2	2	77.58
2	1	2	1	1	2	1	2	87.94
3	2	2	1	2	1	1	1	71.78
4	2	1	2	1	2	1	1	72.14
5	2	1	1	1	1	2	2	87.15
6	1	1	2	2	1	1	2	86.57
7	1	1	1	2	2	2	1	84.03
8	1	2	2	1	1	2	1	77.96

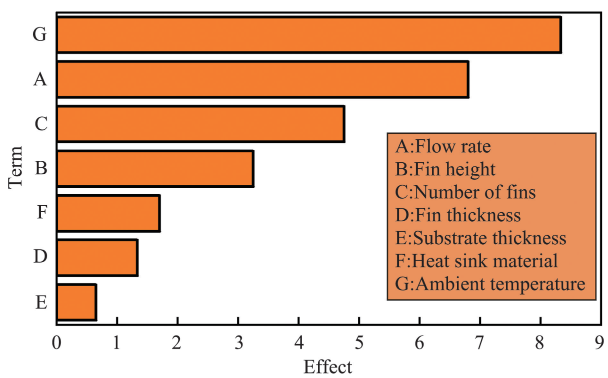

Fig. 7 Degree of influence of various factors

Through orthogonal test design, it can be known that flow rate and ambient temperature are the most significant factors affecting the heat dissipation characteristics of the finned heat sink, followed by the number of fins, fin height, heat sink material, and fin thickness, while the effect of substrate thickness is minimal. Based on the analysis above, the substrate thickness is chosen to be 24 mm. Since the environmental temperature and coolant flow rate cannot be changed through structural design, this paper limits the factors for optimization design to the number of fins N, fin height h, and fin thickness δ. Based on the analysis in Section 1, the constraint range of these three factors is established as follows:

$$77 \leqslant N \leqslant 81$$
$$2.5 \text{ mm} \leqslant \delta \leqslant 4.0 \text{ mm}$$
$$40 \text{ mm} \leqslant h \leqslant 55 \text{ mm}$$

3.2 Response surface methodology design

Response surface methodology design based on limited factors and intervals can reduce the workload. In this paper, the design variables are set as the number of fins N, fin height h, and fin thickness δ, while the maximum temperature T_{max} of the IGBT module is the response variable. A response surface model is established, and level of each design variable is encoded with (-1, 1). Table 4 lists each design variable's encoded values and their corresponding levels.

Table 4 Coding and level of each design variable

Factor	Variable	-1	1
Number of fins	N	77	81
Fin height	h	40 mm	55 mm
Fin thickness	δ	2.5 mm	4.0 mm

This paper uses box-behnken design (BBD) method for the response surface optimization design, since the response surface model adopts three factors and two levels of experimental design. Based on the value ranges of each design variable, researchers created an experimental design plan and simulated each group of schemes. The final simulation results are shown in Table 5.

Table 5 Test scheme and simulation results

Program	Fin height/mm	Number of fins	Fin thickness/mm	Maximum temperature/℃
1	40.00	80	2.94	73.60
2	42.50	76	2.81	72.00
3	45.00	82	2.75	68.30
4	46.88	78	2.63	68.70
5	48.43	80	3.52	67.58
6	48.75	76	3.31	72.00
7	49.38	82	4.00	69.74
8	50.00	76	2.50	74.00
9	51.25	78	3.25	67.39
10	51.88	82	2.69	65.80
11	52.50	80	2.56	66.20
12	53.13	76	3.88	69.00
13	53.75	82	3.44	67.89
14	53.38	80	3.94	67.34
15	55.00	76	3.00	71.80

Researchers performed a multivariate nonlinear regression analysis on the design variables, including the number of fins N, fin height h, and fin thickness δ, according to the principle of response surface methodology. The response surface model for the relationship between the design variables and the maximum temperature T_{max} is obtained. The model is as follows.

$$T_{max} = 3068.59662 - 1.41329h - 69.85930N - 100.71739\delta - 0.063771hN - 0.015245h\delta + 1.00558N\delta + 0.06484h^2 + 0.43478N^2 + 3.255448\delta^2 \quad (13)$$

Rewrite Eq. (13) into the standard response surface polynomial form:

$$T_{max} = 3068.59662 - 1.41329x_1 - 69.8593x_2 - 100.71739x_3 - 0.063771x_1x_2 - 0.015245x_1x_3 + 1.00558x_2x_3 + 0.06484x_1^2 + 0.43478x_2^2 + 3.25544x_3^2 \quad (14)$$

where, x_1 is the height of fins (h), x_2 is the number of fins (N), x_3 is the thickness of fins (δ).

The response surface figures for each design variable are plotted based on Eq. (14), as shown in Figs 8, 9 and 10. These figures intuitively depict the impact of interaction effects among the design variables on the response surface function values.

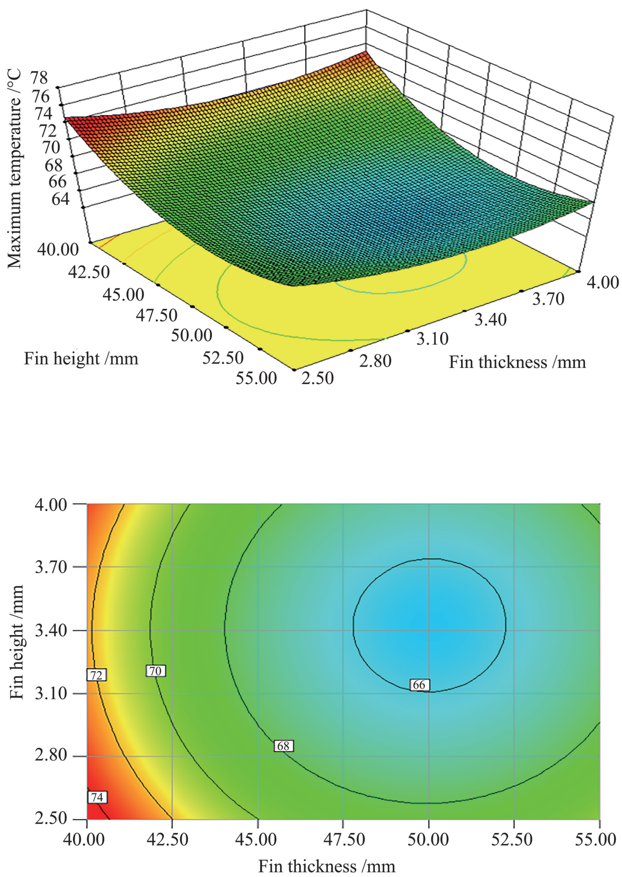

Fig. 8 Response surface and isotherm plot under the interaction of the height and thickness of fins

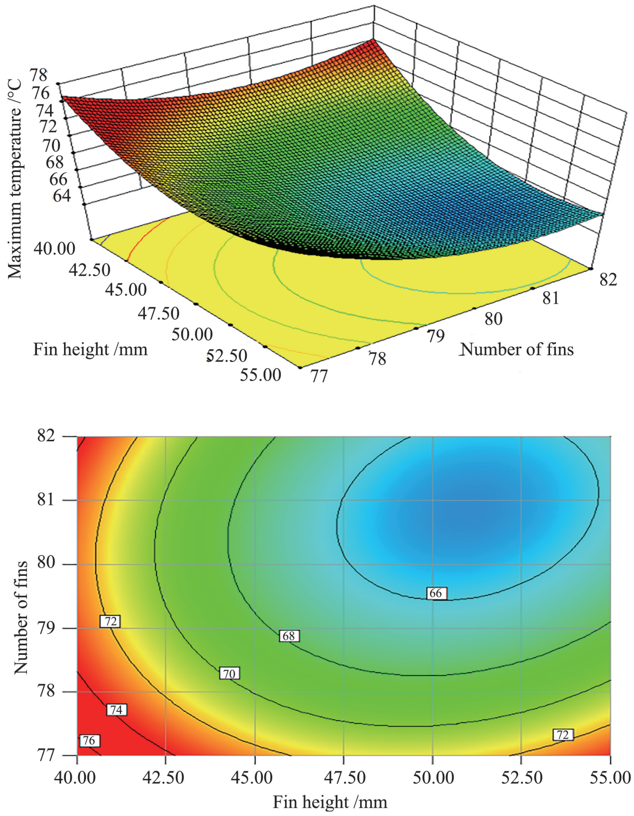

Fig. 9 Response surface and isotherm plot under the interaction of the height and number of fins

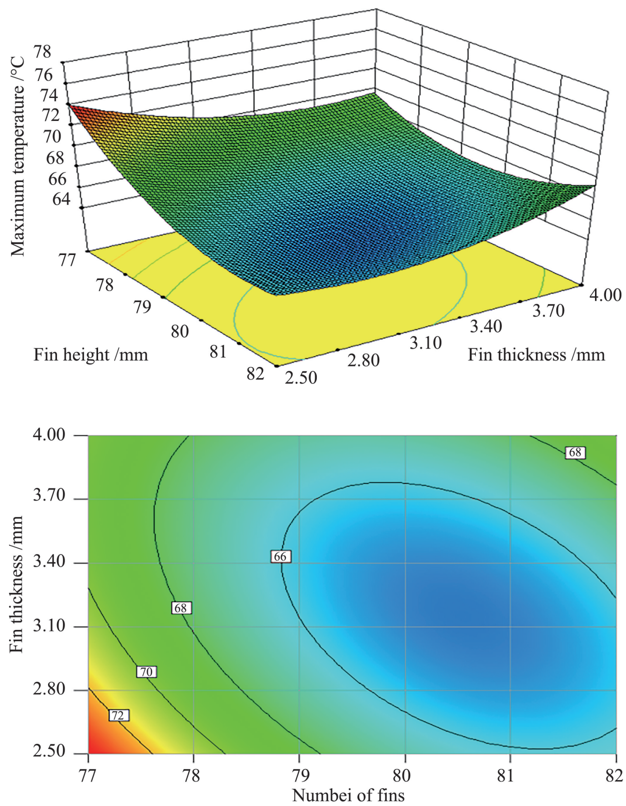

Fig. 10 Response surface and isotherm plot under the interaction of the number and thickness of fins

The optimized design scheme obtained through the response surface function is presented in Table 6. It can ensure that the maximum temperature of the IGBT module reaches 65.75 ℃ when it reaches steady-state, which is 11.23 ℃ lower than the initial design scheme and meets the design requirement of not exceeding 68.00 ℃.

Table 6 Comparison of optimization results

Program	Fin height/mm	Fin thickness/mm	Number of fins	Maximum temperature/℃
Before optimization	45.00	2.00	80	76.98
Optimized	48.13	3.38	81	65.75

4 Experimental verification

Based on the above liquid cooling scheme and its optimized results, researchers constructed a set of prototypes and conducted heat dissipation tests on a motor drag test bench. The test bench consisted of four parts: the dragging system, control system, detection system, and cooling system, as shown in Fig. 11. The testing and on-site debugging are illustrated in Fig. 12.

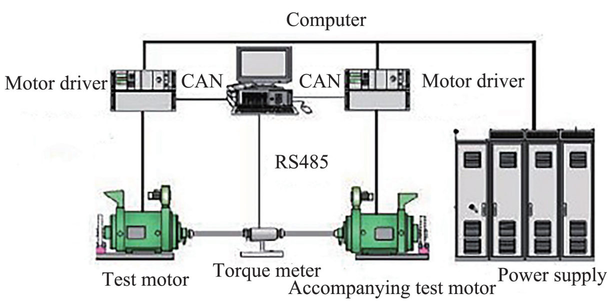

Fig. 11 Composition of the motor drag test bench

Fig. 12 Motor load test and commissioning diagram on site

The experiment involves the following specific steps.

(1) Start the air conditioner before the experiment and set the ambient temperature to 45 ℃ to simulate the temperature of the outdoor port. Start the experiment once the temperature stabilizes.

(2) Start the upper computer to collect and record temperature changes.

(3) Start the motor and run it for a period of time under preset load conditions to eliminate other extraneous factors. Then, run the AGV motor driver continuously at 35%, 70%, 85%, and 100% load rates. Collect relevant test data when the load rate reaches 100%. The IGBT junction temperature curve is shown in Fig. 13.

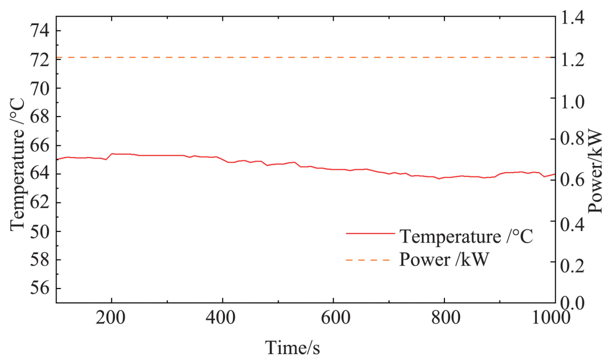

Fig. 13 IGBT junction temperature and power curve

Fig. 13 indicates that the IGBT junction temperature can reach the expected temperature value, and the temperature fluctuation is slight, which confirms the effectiveness of the proposed liquid cooling scheme and its optimization results.

5 Conclusion

This paper proposes a liquid cooling scheme for the heavy-duty AGV motor driver in port environment, and improves the heat dissipation effect by analyzing and optimizing the core heat dissipation component——the finned heat sink. The main work and conclusions are as follows.

(1) The temperature distribution of the initial scheme is studied using Fluent software, exploring the influence of the structural parameters of the finned heat sink on the junction temperature of the IGBT module, and obtaining the range of structural parameter values with the best heat dissipation effect.

(2) A mathematical heat transfer model of the fin is established, and the influence of structural parameters on heat transfer characteristics is studied through numerical analysis.

(3) An orthogonal test is used to analyze the primary and secondary factors affecting the finned heat sink's heat transfer characteristics. The response surface method is used to solve the multi-parameter combination optimization problem, resulting in a 14.57% enhancement of the heat dissipation effect. Finally, the validity of this paper's research is verified through experiments.

This paper provides valuable insights and guidance for the heat dissipation problems of high-power IGBT modules and heat sinks.

References

[1] DE R M, VERSTEYHE M, DEBROUWERE F. Automated guided vehicle systems, state-of-the-art control algorithms and techniques [J]. Journal of Manufacturing Systems, 2020, 54: 152-173.
[2] VIS I F. Survey of research in the design and control of automated guided vehicle systems [J]. European Journal of Operational Research, 2006, 170(3): 677-709.
[3] YAN R, DUNNETT S J, JACKSON L M. Novel methodology for optimising the design, operation and maintenance of a multi-AGV system [J]. Reliability Engineering and System Safety, 2018, 178: 130-139.
[4] JANICKI M, NAPIERALSKI A. Modelling electronic circuit radiation cooling using analytical thermal model [J]. Microelectronics Journal, 2000, 31(9-10): 781-785.
[5] BAHMAN A S, BLAABJERG F. Optimization tool for direct water cooling system of high power IGBT modules[C] // Proceedings of the 2016 18th European Conference on Power Electronics and Applications. Karlsruhe, Germany: IEEE, 2016: 1-10.
[6] KHOSHVAGHT-ALIABADI M, HASSANI S, MAZLOUMI S H. Comparison of hydrothermal performance between plate fins and plate-pin fins subject to nanofluid-cooled corrugated miniature heat sinks [J]. Microelectronics Reliability, 2017, 70: 84-96.
[7] LI W, LI G, SUN Z, et al. Real-time estimation of junction temperature in IGBT inverter with a simple parameterized power loss model [J]. Microelectronics Reliability, 2021, 127: 114409.
[8] SATHE A, GAIKWAD A, SANAP S. A design approach for thermal enhancement in heat sinks using different types of fins: a review [J]. Frontiers in Thermal Engineering, 2023, 2: 1-13.
[9] FENG X. Investigation on the optimization of heat transfer of fin heat sink applied in cob light source [D]. Jinan: Shandong University, 2021. (In Chinese)
[10] ZHANG Y M, DENG E P, ZHAO Z B. Research overview of multi-physical field coupling in the package of crimped IGBT devices [J]. Proceedings of the CSEE, 2019, 39(21): 14.
[11] HUO Y, RAO Z, LIU X, et al. Investigation of power battery thermal management by using mini-channel cold plate [J]. Energy Conversion Management, 2015, 89: 387-395.
[12] XU Y, BAO J, NING R, et al. Heat dissipation simulation of double-sided liquid-cooled IGBT module package [C] // Proceedings of the 2019 20th International Conference on Electronic Packaging Technology. Hong Kong, China: IEEE, 2019: 1-4.
[13] XIAHOU G, MA R, ZHANG J J, et al. Thermal performance of an array condenser flat heat pipe for IGBT heat dissipation [J]. Microelectronics Reliability, 2020, 104: 113546.
[14] SONG Q G, WANG Q, ZHANG C, et al. Multi-objective optimization of a water-cooled heatsink based on ANSYS analysis [J]. Fluid Machinery, 2022, 50(4): 65-70. (In Chinese)
[15] LAMPIO K, KARVINEN R. Optimization of convectively cooled heat sinks [J]. Microelectronics Reliability, 2017, 79: 473-479.
[16] ALBRECHT P. A new theoretical approach to Runge-Kutta methods [J]. SIAM Journal on Numerical Analysis, 1987, 24(2): 391-406.
[17] BOLBOACĂ S D, JÄNTSCHI L. Design of experiments: Useful orthogonal arrays for number of experiments from 4 to 16 [J]. Entropy, 2007, 9(4): 198-232.
[18] COCHRAN W G, COX G M. Experimental designs[M]. 2nd. Oxford: John Wiley & Sons, 1957.
[19] FERREIRA S C, BRUNS R, FERREIRA H S, et al. Box-Behnken design: an alternative for the optimization of analytical methods [J]. Analytica Chimica Acta, 2007, 597(2): 179-186.
[20] LI X, HAO J. Orthogonal test design for optimization of synthesis of super early strength anchoring material [J]. Construction and Building Materials, 2018, 181: 42-48.
[21] LIN R, DIAO X, MA T, et al. Optimized microporous layer for improving polymer exchange membrane fuel cell performance using orthogonal test design [J]. Applied Energy, 2019, 254: 113714.
[22] RENJIE L. Orthogonal test design for optimization of the extraction of polysaccharides from Phascolosoma esulenta and evaluation of its immunity activity [J]. Carbohydrate Polymers, 2008, 73(4): 558-563.
[23] ZHAO N Z, LEI Y, ZHAO Y S, et al. Multi-factor analysis of reflection from granite surfaces [J]. Journal of China University of Mining Technology, 2007, 17(2): 255-257. (In Chinese)

LIU Xuan, born in 1980. She received her Ph. D degree from the College of Mechanical Engineering of Hebei University of Technology in 2010, her M. S. degree from Hebei University of Technology in 2007 and her B. S. degree from Agricultural University of Hebei in 2004. She has been engaged in the basic research and application development of robot mechanism and control, human-machine integration technology, automotive electronics technology and so on.